Journal of
Nanoscience and Nanotechnology
Vol. 9, 7388–7392, 2009

Doping Effect of CNT and Nano-Carbon in Magnesium Diboride Bulk

Jun Hyung Lim[1], Chang Min Lee[1], Jin Hyun Park[1], Jun Hyuk Choi[1], Jong Hyun Shim[1], Jinho Joo[1,*], Young Hee Lee[2], Won Nam Kang[3], and Chan-Joong Kim[4]

[1] *School of Advanced Materials Science and Engineering, Sungkyunkwan University, Suwon, 440-746, Korea*
[2] *Institute of Basic Science, Center for Nanotubes and Nanostructured Composites, Sungkyunkwan University, Suwon, 440-746, Korea*
[3] *Department of Physics, Sungkyunkwan University, Suwon, 440-746, Korea*
[4] *Nuclear Nanomaterials Development Laboratory, Korea Atomic Energy Research Institute, Daejeon, 305-353, Korea*

We fabricated carbon nanotube (CNT)- and nano-carbon (NC)-doped MgB_2 using an *in-situ* process in order to improve the critical current density (J_c) at high magnetic field. We then evaluated the effects of the doped carbon content on phase formation, microstructure, and critical properties. CNT had a diameter and length of 5–10 nm and 0.5–1 μm, respectively, and NC was a sphere with a diameter of 5–30 nm. The bulk $MgB_{2-x}C_x$ samples with $x = 0$, 0.05, and 0.1 for NC and CNT were fabricated by pressing into pellets and then sintered at 900 °C for 30 min. NC was more effective than CNT for carbon doping at the B site in MgB_2 and, therefore, the NC-doped MgB_2 samples had a lower critical temperature (T_c) of 35.0–34.7 K than that of the CNT-doped samples (36.4–36.1 K). In addition, the J_c(B) behavior was improved when NC and CNT were doped due to doping effect. Microstructural observation suggested that the nano-sized and unreacted NC particles and the nanodomain MgB_2 acted as effective flux pinning centers for the NC- and CNT-doped MgB_2, respectively.

Keywords: Carbon Nanotube, Critical Current Density, *In-Situ* Process, MgB_2, Nano-Carbon.

1. INTRODUCTION

Due to its relatively high critical temperature (T_c), large coherence length, and low material cost, MgB_2 is a promising material for large-scale applications. However, the critical current density (J_c) of MgB_2 is significantly degraded in high magnetic fields because of its weak pinning centers and low upper critical field (H_{c2}). It has recently been reported that the enhancement effect of various chemical dopants on the J_c in high magnetic fields has been examined. Carbon-based materials such as SiC,[1] B_4C,[2] diamond,[3] graphite,[4] nano-carbon (NC),[5,6] and carbon nanotube (CNT)[7,8] have been examined as effective doping elements. Substantial studies have been dealt with SiC and B_4C as dopant due to their potential for the improvement of J_c performance at high magnetic field (J_c(B)). In addition, CNTs are interesting because of their geometry with high aspect ratio while NC is also attractive due to its low decomposition temperature and cost. We previously studied the effect of NC doping on critical properties, and confirmed the effectiveness of NC doping in bulk MgB_2 to improve the J_c(B) behavior.[5] We expected that NC might play one, or possibly both, of two different roles: electron scattering centers as the dopant in the lattice or nano-sized inclusions as pinning centers. However, we were unable to determine the doping mechanism due to the lack of microstructural evidence. Similarly, CNTs might play both of the roles,[8] but the effect of remained (unreacted) CNTs on microstructure and resultant J_c(B) behavior has not been clearly understood.

In a systematic extension to our previous study, therefore, we selected single-wall CNT with a relatively high decomposition temperature and NC in order to characterize the roles of these two dopants. We fabricated $MgB_{2-x}C_x$ ($x = 0$, 0.05, and 0.1) bulk samples and evaluated the effect of doping on the phase formation, microstructure, T_c, and J_c. In addition, the microstructure was characterized by the scanning electron microscopy (SEM) and transmission electron microscopy (TEM) and correlated with the critical properties.

*Author to whom correspondence should be addressed.

 1533-4880/2009/9/7388/005 doi:10.1166/jnn.2009.1756

2. EXPERIMENTAL DETAILS

In order to evaluate the effect of NC and CNT additions on the microstructure and critical properties, we fabricated the bulk MgB_2 using a conventional powder metallurgy technique combined with *in-situ* reaction. Magnesium (Tangshan, 325 mesh, 99.9%), amorphous boron (Tangshan, 4–6 μm, 99.9%), and either NC (TIMCAL, 99%) or CNT (Iljin CNT) powders were used to make the nominal compositions of $MgB_{2-x}C_x$ with $x = 0$, 0.05, and 0.1. The ingredient powders were loaded into a jar in appropriate proportions and mixed by hand mixing method for 10 min in an Ar atmosphere in glove box. Subsequently, the mixtures were put in a plastic container, sealed in an Ar atmosphere, and agitated supersonically for 1 hr. Figure 1 shows the TEM micrographs of the as-received NC and CNT showing that the NC were sphere with a diameter of 5–30 nm and the CNT were shaped as rods with a diameter of 5–10 nm and length of 0.5–1 μm. The sample of $x = 0$, 0.05, and 0.1 in $MgB_{2-x}C_x$ prepared by mixing of NC or CNT is hereafter denoted as the undoped, 0.05 NC, 0.1 NC, 0.05 CNT, and 0.1 CNT samples, respectively. The mixed powders were pressed into pellets, 10 mm in diameter and 1.5 mm in thickness, under a uniaxial pressure of 500 MPa and then the compacts were sealed in a Ti tube and sintered at 900 °C in a flowing Ar gas (99.9%).

The crystalline structure and phase formation were examined by powder X-ray diffraction (XRD) using a BRUKER (D8 Discover) diffractometer with CuK_α radiation. The change in lattice parameters was calculated from the (002) and (100) peaks and confirmed using the EVA® program based on Rietveld refinement analysis. The grain morphology and microstructure were also examined by SEM and TEM (JEM 3010). The magnetic J_c and T_c values were derived from the height of the magnetization loop using Bean's model. The magnetization of the samples was measured at a temperature of 5 and 20 K using a magnetic property measurement system (MPMS, Quantum design) in a time-varying magnetic field and amplitude up to 5 T.

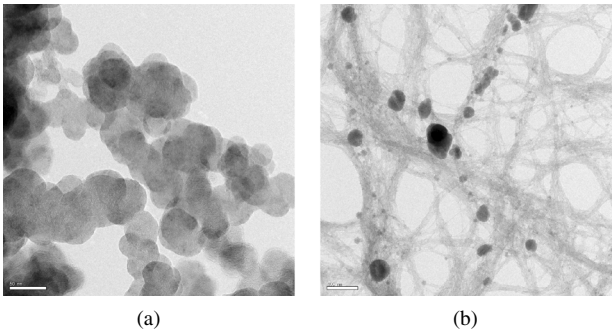

(a) (b)

Fig. 1. TEM micrographs of (a) NC and (b) CNT.

3. RESULTS AND DISCUSSION

Figure 2(a) shows the XRD patterns of the undoped MgB_2 and doped $MgB_{2-x}C_x$ samples sintered at 900 °C. All samples comprised MgB_2 as the major phase with MgB_4 and MgO as secondary phases. No peak related to carbon appeared in any of the sample patterns, probably because the NC and CNT particle sizes were too small for XRD detection. For the undoped sample, the amounts of MgB_4 and MgO phases were increased in comparison with those for the doped samples. The MgO phase is well formed at high sintering temperature and MgO formation produces a Mg-deficient phase, MgB_4, in the Mg-B binary system. The smaller amount of these secondary phases in the CNT- and NC-doped samples was due to oxygen absorption of CNT and CO_2 formation by reaction between oxygen and NC, respectively.[9] There was no marked difference between the XRD patterns of the CNT- and NC-doped samples.

The variations of the *a*- and *c*-axes in the MgB_2 with a nominal carbon content were measured from the XRD patterns and the peaks of the (002) and (100) planes were magnified in Figure 2(b). The 2θ value of the (100) peak was shifted from 33.60° for the undoped sample to 33.63° and 33.64° for the 0.05 and 0.1 CNT samples, and to 33.72° and 33.73° for the 0.05 and 0.1 NC samples, respectively. In contrast, the (002) peak remained nearly unchanged for all samples.

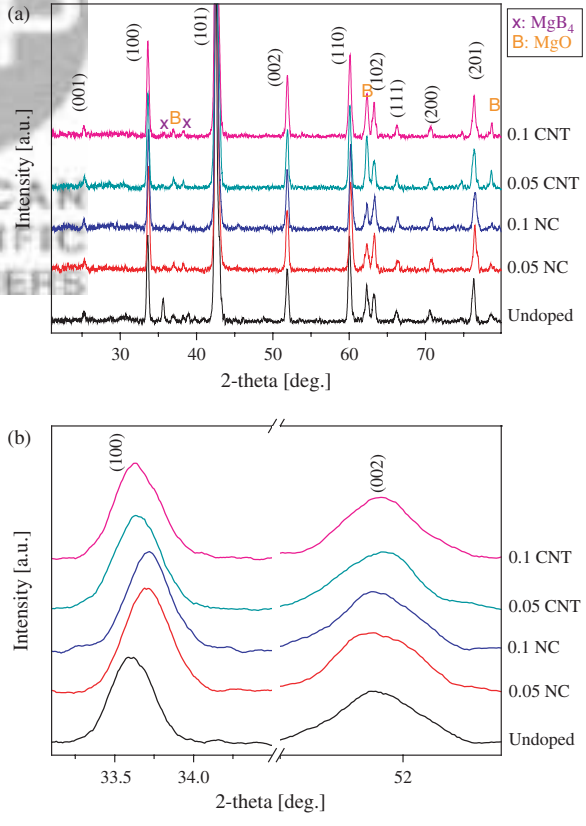

Fig. 2. (a) XRD patterns of the undoped and doped $MgB_{2-x}C_x$ and (b) their magnified peaks of the (002) and (100) planes.

The lattice parameters were obtained from the 2θ values using the Rietveld refinement analysis. The a-axis lattice parameter decreased from 3.0871 Å for the undoped sample to 3.0813 Å and 3.0799 Å for the 0.05 and 0.1 CNT samples and 3.0730 Å and 3.0711 Å for the 0.05 and 0.1 NC samples, respectively. The decrease was more significant for the NC-doped samples than for the CNT-doped samples. On the other hand, the c-axis lattice parameter was nearly constant for all the samples and remained in the range of 3.5231 Å–3.5248 Å. It is generally accepted that the a-axis shrinks when carbon is substituted for the B site due to the differences of their atomic size and number of valence electrons. Our result is in good agreement with the reports of other groups,[3–8] indicating that carbon is substituted in the B honeycomb layer and does not change the interlayer distance in the MgB_2 crystal. In addition, the content of carbon substitution for the B site in the NC sample was larger than that in the CNT sample because the a-axis for the former sample contracted more than the latter, which was attributed to the lower decomposition temperature range of NC (150–700 °C) than that of CNT (750–1000 °C).

Figure 3 shows the SEM micrographs of the fractured surface of the undoped, 0.1 NC, and 0.1 CNT samples. All the samples had similar morphology, size and number of "Kirkendall voids." These voids were formed due to the diffusion at around 650 °C of melted Mg into amorphous B, forming MgB_2. As can be seen in Figure 3(a), the MgO particles were formed mostly at the inner void surface for the undoped sample and its size was in the range of 83–143 nm. MgO particles of several tens of nanometer size cannot improve the flux pinning effect because the coherence length of MgB_2 is 6–7 nm.

On the other hand, MgO was not well observed in significant amount in the doped samples, which is consistent with the aforementioned XRD analysis result indicating that the MgO amount was decreased in the doped samples probably due to that the CNT and NC play role of 'oxygen getter,' as noted earlier. Carbon was detected in the entire region of all the doped samples by energy dispersive X-ray (EDX) analysis. The microstructure of the 0.1 CNT sample is shown in Figure 3(d) at high magnification (×100,000). It was observed that CNTs interlink the MgB_2 grains, which can improve the connectivity between grains and be advantageous for the porous microstructure of *in-situ* MgB_2.

Figure 4 shows the T_c values and the magnetic dependence of J_c at 5 and 20 K for the undoped and doped samples. From Figure 4(a), the T_c (onset 10%) decreased from 37.0 K for the undoped MgB_2 to 36.4 K and 36.1 K for the 0.05 and 0.1 CNT samples and 35.0 K and 34.7 K for the 0.05 and 0.1 NC samples, respectively, indicating that T_c decreased with increasing nominal carbon content and that the NC samples had lower T_c values than the CNT samples did. This behavior was similar to the changes of the

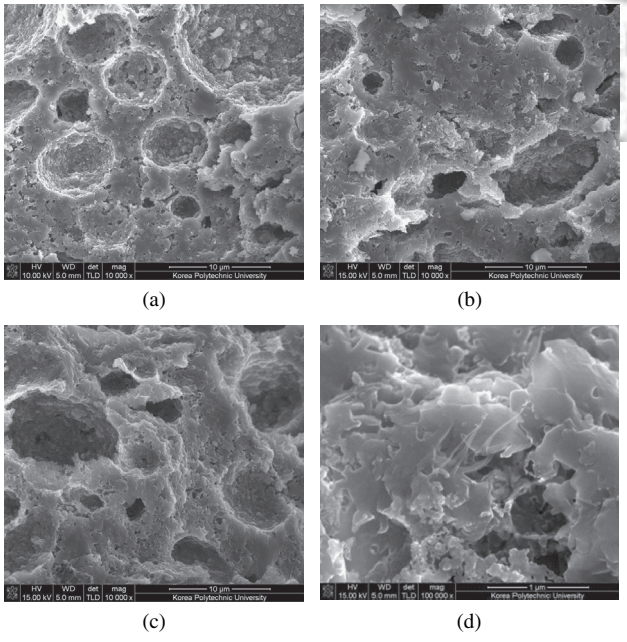

Fig. 3. SEM micrographs of the fractured surface of the (a) undoped, (b) 0.1 NC-, and (c) 0.1 CNT-doped samples, and (d) a highly magnified image (×100,000) of (c).

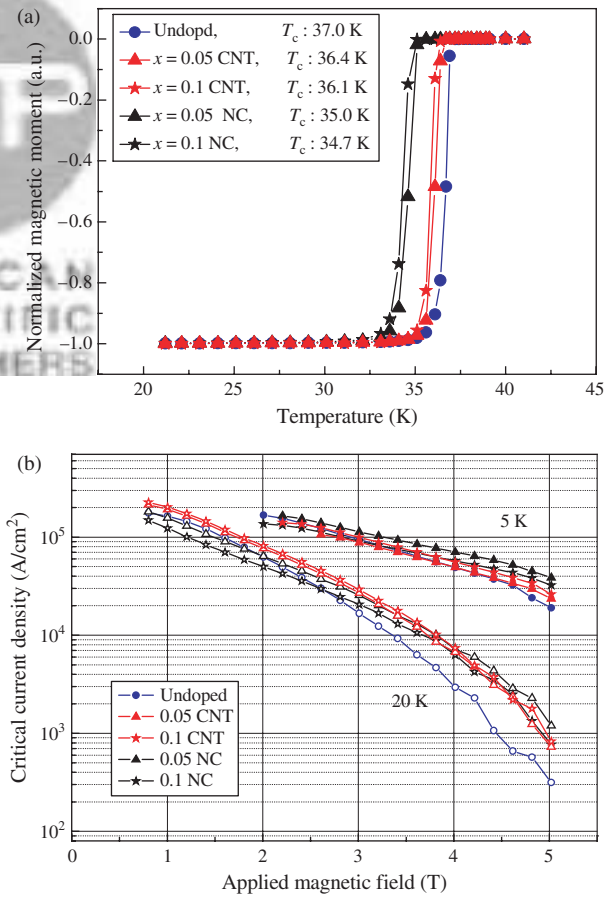

Fig. 4. T_c and J_c(B) behavior at 5 and 20 K for the undoped and doped samples.

a-axis lattice parameter from the XRD analysis. In view of the fact that the reduction of T_c values originated from the increased electron concentration in the MgB_2 structure,[10] the larger decrease of T_c for the NC samples was related to their higher doping contents than for the CNT samples.

Figure 4(b) shows the J_c(B) behaviors at 5 and 20 K in an applied magnetic field up to 5 T. For all samples, the J_c values decreased with increasing magnetic field and this decrease was more rapid for the undoped sample than for the doped samples at 5 and 20 K. At 5 K, the J_c of the undoped sample had a crossover at approximately 3.2 T, 3.5 T, and 2.6 T for the 0.1 NC, 0.05 CNT, and 0.1 CNT samples, respectively. Above 3.5 T, all doped samples exhibited higher J_c than the undoped sample and the 0.05 NC sample gave the best J_c in all magnetic fields at 5 K. The superior J_c(B) behavior of the doped samples compared to the undoped sample was attributed to the combined effects of excess electrons and lattice distortion because decomposed carbon is partially substituted into the B site for the former.

At 20 K, the J_c of the CNT samples was the highest at 0.8 T, but a crossover in the J_c value occurred at approximately 3.5 T and 4.0 T for the 0.05 NC and 0.1 NC samples, respectively. Furthermore, the J_c(B) behavior was nearly comparable for the CNT and NC samples, although the doping content for the former was significantly smaller, as shown in the XRD analysis. This result led us to assume that another mechanism also contributed to the improved J_c(B) behavior for the CNT sample.

Therefore, TEM observations were conducted for both the 0.1 doped samples, as shown in Figure 5. In the 0.1 NC sample, the NC was located either at the grain boundary (Fig. 5(a)) or at surface of the porous MgB_2 structure (Fig. 5(b)). The size of NC ranged from 5–30 nm, enabling it to act as an effective pinning center. Thus, the enhanced flux pinning was partly attributed to the high density of these NC inclusions.

Figures 5(c and d) show the microstructure of the 0.1 CNT sample. CNT was 'embedded'[11] along the MgB_2 grain surface, as can be seen in Figure 5(c). The formation of the 'embedded morphology' was attributed to the CNT motion during the MgB_2 reaction. The MgB_2 phase is generally formed through the liquid state diffusion of Mg into amorphous B. During the reaction, a CNT moves slightly along the direction of liquid Mg flux while maintaining good contact with Mg and B, so that CNT is embedded along the MgB_2 after the reaction is completed. In addition, MgB_2 nanodomains were observed at the interface between MgB_2 and CNT. Dou et al. reported that MgB_2 formed along CNTs because they act as the nucleation centers.[10] The nanodomain formation is probably explained as follows. Dislocations can be generated due to the mismatch between graphene and MgB_2 during the formation and growth of MgB_2. These dislocation

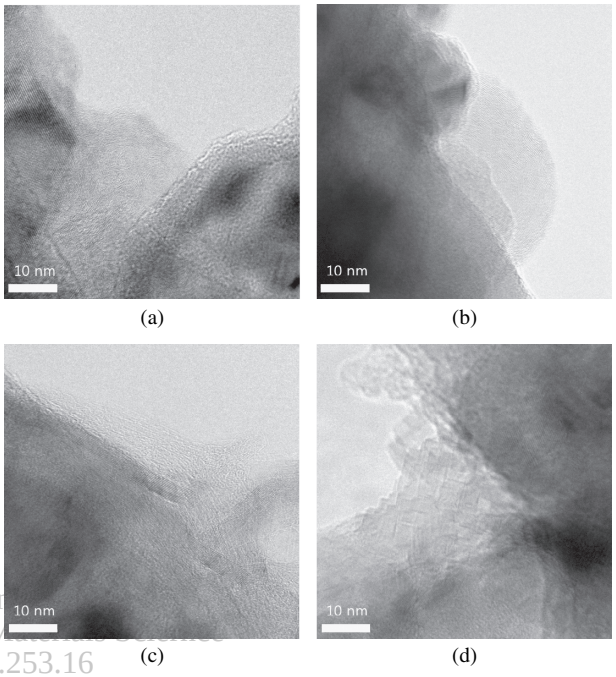

Fig. 5. TEM micrographs of the (a) and (b) 0.1 NC and (c) and (d) 0.1 CNT samples.

piles migrate and rearrange their locations in a pattern of so-called low-energy dislocation structure (LEDS) in order to minimize the strain energy. These rearranged dislocation piles may produce a low-angle nanodomain. We considered that these nano-grain boundaries also act as an effective pinning center, thus enhancing the J_c(B) behavior of the doped samples relative to the undoped sample at high magnetic field.

4. CONCLUSIONS

We fabricated the CNT- and NC-doped MgB_2 samples to improve their J_c(B) behavior and then correlated the microstructural evolution to the observed critical properties. The T_c values were lower for the NC samples (35.0–34.7 K) than for the CNT samples (36.4–36.1 K) because more carbon was doped into MgB_2 in the former, probably due to the lower decomposition temperature range for NC.

The doped samples exhibited higher J_c values at high magnetic field than the undoped sample did. The superior J_c(B) behavior for the NC samples was partly attributed to the carbon doping effect on B and the existence of the nano-sized and unreacted NC particles. On the other hand, the J_c(B) behavior was nearly comparable among the CNT and NC samples, despite the significantly smaller doping content for the former. We believed that the formation of nanodomain MgB_2 near CNT, due to the mismatch between CNT and MgB_2, probably acted as an effective flux pinning center, based on the TEM study results.

Acknowledgments: This research was supported by a grant (R-2006-1-248) from Electric Power Industry Technology Evaluation and Planning (ETEP), Republic of Korea.

References and Notes

1. S. X. Dou, S. Soltanian, J. Horvat, X. L. Wang, S. H. Zhou, M. Ionescu, H. K. Liu, P. Monroe, and M. Tomsic, *Appl. Phys. Lett.* 81, 3419 (**2002**).
2. R. A. Ribeiro, S. L. Bud'ko, C. Petrovic, and P. C. Canfield, *Physica C* 384, 227 (**2003**).
3. Y. Zhao, C. H. Cheng, X. F. Rui, H. Zhang, P. Munroe, H. M. Zeng, N. Koshizuka, and M. Murakami, *Appl. Phys. Lett.* 83, 2916 (**2005**).
4. B. J. Senkowicz, J. E. Giencke, S. Patnaik, C. B. Eom, E. E. Hellstrom, and D.C. Larbalestier, *Appl. Phys. Lett.* 86, 202502 (**2005**).
5. J. H. Lim, K. T. Kim, E. C. Park, C. M. Lee, J. H. Shim, J. Joo, W. N. Kang, and C. J. Kim, *Physica C* 468, 1379 (**2008**).
6. W. K. Yeoh, J. H. Kim, J. Horvat, X. Xu, M. J. Qin, S. X. Dou, C. H. Jiang, T. Nakane, H. Kumakura, and P. Monroe, *Supercond. Sci. Technol.* 19, 596 (**2006**).
7. S. X. Dou, W. K. Yeoh, J. Horvat, and M. Ionescu, *Appl. Phys. Lett.* 83, 4996 (**2003**).
8. W. K. Yeoh, J. Horvat, S. X. Dou, and V. Keast, *Supercond. Sci. Technol.* 17, S572 (**2004**).
9. K. Seo, C. Kim, Y. S. Choi, K. A. Park, Y. H. Lee, and B. Kim, *J. Am. Chem. Soc.* 125, 13946 (**2005**).
10. S. Lee, T. Masui, A. Yamamoto, H. Uchitama, and S. Takama, *Physica C* 397, 7 (**2003**).
11. S. X. Dou, W. K. Yeoh, O. Shcherbakova, D. Wexler, Y. Li, Z. M. Ren, P. Munroe, S. K. Chen, K. S. Tan, B. A. Glowacki, and J. L. MacManus-Driscoll, *Adv. Mater.* 18, 785 (**2006**).

Received: 14 October 2008. Accepted: 21 February 2009.